J. Astrophys. Astr. (2006) **27,** 115–124

Spectroscopic Studies of Solar Corona VI: Trend in Line-width Variation of Coronal Emission Lines with Height Independent of the Structure of Coronal Loops

Jagdev Singh[1,*], Takashi Sakurai[2], Kiyoshi Ichimoto[2] & S. Muneer[3]
[1]*Indian Institute of Astrophysics, Koramangala, Bangalore 560 034, India.*
[2]*National Astronomical Observatory of Japan, 2-21-1, Ohsawa, Mitaka, Tokyo, 181-8588, Japan.*
[3]*Vainu Bappu Observatory, Indian Institute of Astrophysics, Kavalur 635 701, India.*
[*]*e-mail: jsingh@iiap.res.in*

Abstract. We have obtained spectroscopic observations in coronal emission lines by choosing two lines simultaneously, one [Fe X] 6374 Å and the other [Fe XI] 7892 Å or [Fe XIII] 10747 Å or [Fe XIV] 5303 Å. We found that in 95 per cent of the coronal loops observed in 6374 Å, the FWHM of the emission line increases with height above the limb irrespective of the size, shape and orientation of the loop and that in case of 5303 Å line decreases with height in about 89 per cent of the coronal loops. The FWHM of 7892 Å and 10747 Å emission lines show intermediate behavior. The increase in the FWHM of 6374 Å line with height is the steepest among these four lines. We have also studied the intensity ratio and ratio of FWHM of these lines with respect to those of 6374 Å as a function height above the limb. We found that the intensity ratio of 7892 Å and 10747 Å lines with respect to 6374 Å line increases with height and that of 5303 Å to 6374 Å decreases with height above the limb. This implies that temperature in coronal loops will appear to increase with height in the intensity ratio plots of 7892 Å and 6374 Å; and 10747 Å and 6374 Å whereas it will appear to decrease with height in intensity ratio of 5303 Å to 6374 Å line *versus* height plot. These findings are up to a height of about 200 arcsec above the limb. The varying ratios with height indicate that relatively hotter and colder plasma in coronal loops interact with each other. Therefore, the observed increase in FWHM with height above the limb of coronal emission lines associated with plasma at about 1 MK may not be due to increase in non-thermal motions caused by coronal waves but due to interaction with the relatively hotter plasma. These findings also do not support the existing coronal loop models, which predict an increase in temperature of the loop with height above the limb.

Key words. Sun: corona—coronal structures—emission line widths—techniques: spectroscopy.

1. Introduction

Temperature variations in the coronal loops may give a clue to the processes responsible to heat up the coronal plasma. The variation in FWHM of coronal emission lines occurs due to two reasons, one because of variation in temperature of the coronal plasma and the other due to variation in the non-thermal velocity. The intensity ratio of a suitable pair of coronal emission line yields information about the temperature of coronal plasma. The line-width of these coronal emission lines may give the non-thermal velocity of the plasma. Most of the time intensity ratios have been studied in EUV lines to determine the temperature and density variations in coronal loops using filter ratio technique (Winebarger *et al.* 2003). Earlier following the discovery (Tousey *et al.* 1973; Vaiana *et al.* 1973) that the hot plasma is contained in closed magnetic structures; Rosner *et al.* (1978) recognized that corona could be approximated as a set of one-dimensional loops that were thermally insulated from the surroundings. They solved the one-dimensional energy balance equation by assuming constant pressure, uniform heating, and a static, semi-circular loop with constant cross section, deriving two scaling laws that related the loop half-length and volumetric heating rate to the resulting high apex temperature and base pressure. Serio *et al.* (1981) extended the scaling laws to allow for non-uniform pressure. Porter & Klimchuk (1995) found that the line-of-sight emission measures of the loops observed with the Soft X-ray Telescope were typically not equal to the emission measures derived from the scaling laws. Kano & Tsuneta (1996) found that temperature and emission measure are the highest at the loop top, and decrease towards the foot-points. They also found that the correlation between the total energy loss and the gas pressure for the steady loops is consistent with the theoretical energy scaling law. From the intensity ratios of various coronal emission lines, Tsubaki (1975) showed the existence of temperature in-homogeneity in the coronal structures. In view of this fact we analysed the simultaneous spectroscopic observations made in coronal emission lines to study the variation of FWHM with height only (Singh *et al.* 1999, 2002, 2003a, 2003b). We found systematic increase in the FWHM of the 6374 Å line and decrease in the FWHM of 5303 Å emission line with height above the limb and small increase in the FWHM of 7892 Å and 10747 Å lines as compared to that of 6374 Å line. The systematic variations and surprising decrease in FWHM of the 5303 Å line with height motivated us to investigate the variation of the intensity ratio, also to determine the temperature variations with height above the limb and found complex variations in the line intensity ratio of coronal emission lines with height above the limb (Singh *et al.* 2004). In this paper we discuss the implications of our findings on the existing coronal loop models.

2. Observations and data analysis

Spectrographic observations of several coronal regions were obtained in the [Fe X] 6374 Å, [Fe XI] 7892 Å, [Fe XIII] 10747 Å and [Fe XIV] 5303 Å emission lines with 25-cm coronagraph at the Norikura Solar Observatory on several days during the years 1997–2004. The Coude type coronagraph provided us coronal image with image scale of 25″ per mm and 7 m focus Littrow type spectrograph formed spectrum with a dispersion of 2.17 Å per mm at the third order red. By choosing different orders for different coronal emission lines, we could observe 6374 Å line in the third order

and 5303 Å line in the fourth order simultaneously by using two CCD cameras. One CCD camera of 512×512 format with pixel size of 13.5×13.5 microns was directly mounted at the focal plan of the Littrow focus and was used to take spectrum around the red line. The second CCD camera of 1024×1024 format with pixel size of 24×24 microns coupled with a 20-cm aperture and 8.86 m focal length Cassegrain telescope was kept in the diffracted beam from the grating which over-spilled the Littrow mirror of the main spectrograph. This camera recorded the spectrum around the green line. Similarly, we could locate the Cassegrain telescope to obtain the red line spectra in the third order and both the infrared lines spectra in the second order simultaneously. We could also make observations in 6374 Å and 7892 Å emission lines simultaneously by locating the Cassegrain telescope at the proper place. The binned CCD camera provided us a dispersion of 31.8 m Å at the green line, 58.4 m Å at the red line, 25 m Å at the 7892 Å and 121 m Å per pixel at infrared lines. But the slit width of 160 microns mostly used to make observations restricted the spectral resolu-

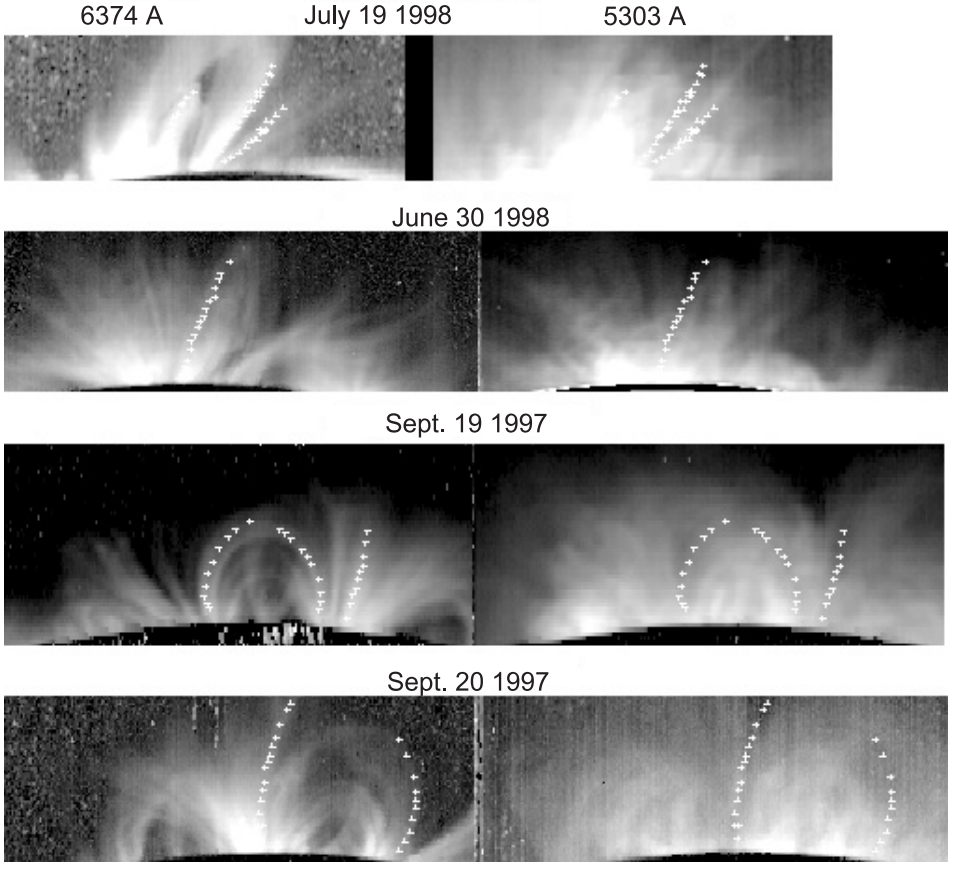

Figure 1. Intensity distribution in the coronal regions observed simultaneously in 6374 Å and 5303 Å coronal emission lines on different days. The + marks indicate the typical examples of different types of coronal loops. The variations in FWHM for both these lines with height above the limb are shown in Fig. 5 for these coronal loops.

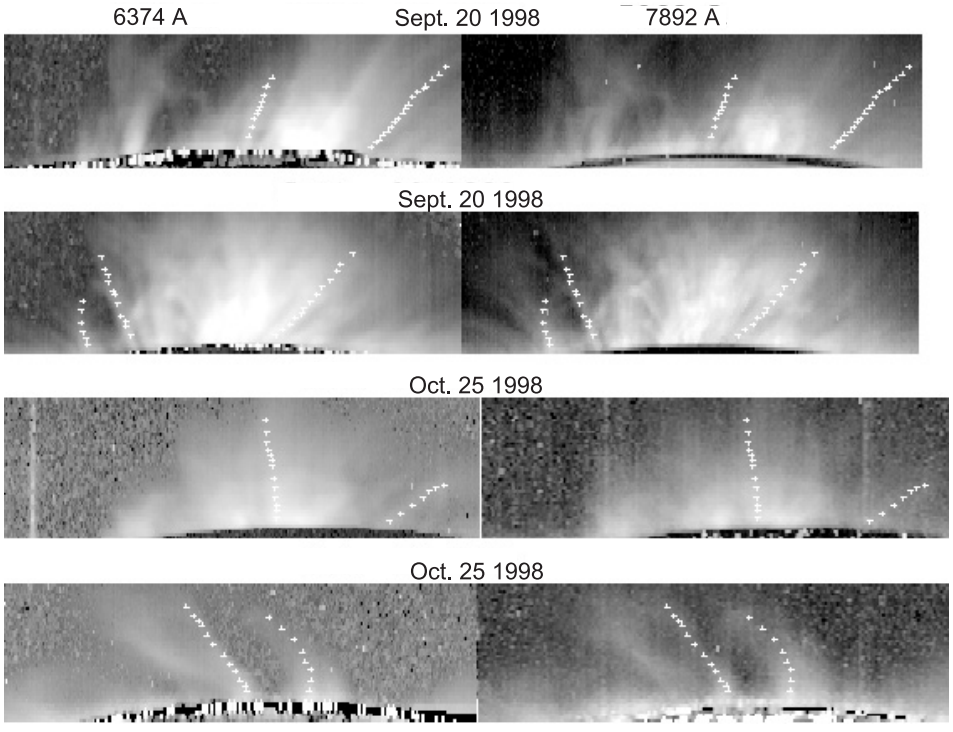

Figure 2. Same as for Fig. 1 but for 6374 Å and 7892 Å emission lines and variations in FWHM for the loops are shown in Fig. 6.

tions to 77 m Å, 128 m Å, 58 m Å and 291 m Å for the green, red, 7892 Å and infrared emission lines respectively and spatial resolution to 4″. The typical exposure time was between 10 and 20 s for the red and green lines depending upon the sky conditions and between 20 and 70 s for the 7892 Å and infrared spectrum. The green and red line spectra were recorded with the same exposure times whereas exposure time for the red line was less compared to the 7892 Å and infrared lines. To maintain the simultaneity in observations, the exposures for both the CCD cameras were started at the same time and the CCD camera for recording the red line spectrum waited till the exposure for the infrared spectrum could be completed to begin the next exposure. The inclination of the glass block installed in front of the entrance slit was changed to obtain the successive spectra at different locations in the solar corona to build a two-dimensional image. One raster scan could be completed in 10–70 minutes depending on the exposure time and the number of steps. The typical raster scan consists of 50 positions with each step of 4″ and covered 200″ × 500″ of the coronal region. All the spectra were corrected for the dark current, flat field and scattered light component due to sky brightness. A Gaussian fit was made to the observed emission line profile at each location of the observed coronal region to compute its peak intensity, central wavelength and width of the emission line. These values were then plotted as a function of spatial locations to obtain spectroheliograms, velocity-grams and width-grams in the these coronal lines. The heliograms, which have different scales due to different

focal lengths of the optics used to image the spectra, were re-scaled and brought on the same spatial scale and dimensions using the solar disc spectrum with three fiducial marks. Figure 1 shows typical examples of heliograms of observed coronal regions on several days in the 6374 Å and 5303 Å lines simultaneously. Figure 2 shows the intensity distribution in some other coronal regions in the 6374 Å and 7892 Å and Fig. 3 shows the coronal regions observed in 6374 Å and 10747 Å emission lines simultaneously. To see the general trend in the parameters of emission lines, we selected 200–300 locations depending upon the area occupied by the coronal structures, with a spatial resolution of $4'' \times 4''$ on all the coronal structures visible in the red line intensity image. The corresponding locations in other images 5303 Å or 7892 Å or 10747 Å were selected automatically using software. Similarly we have done the analysis for individual coronal structures by selecting 10–20 locations depending upon its length to investigate the variations in emission line parameters as a function of height above the limb. To study the variation of line widths of these lines with height above the limb a linear fit to the FWHM data at various locations along the length of the individual coronal loop was made even though the linear fit may not be the best fit to the data.

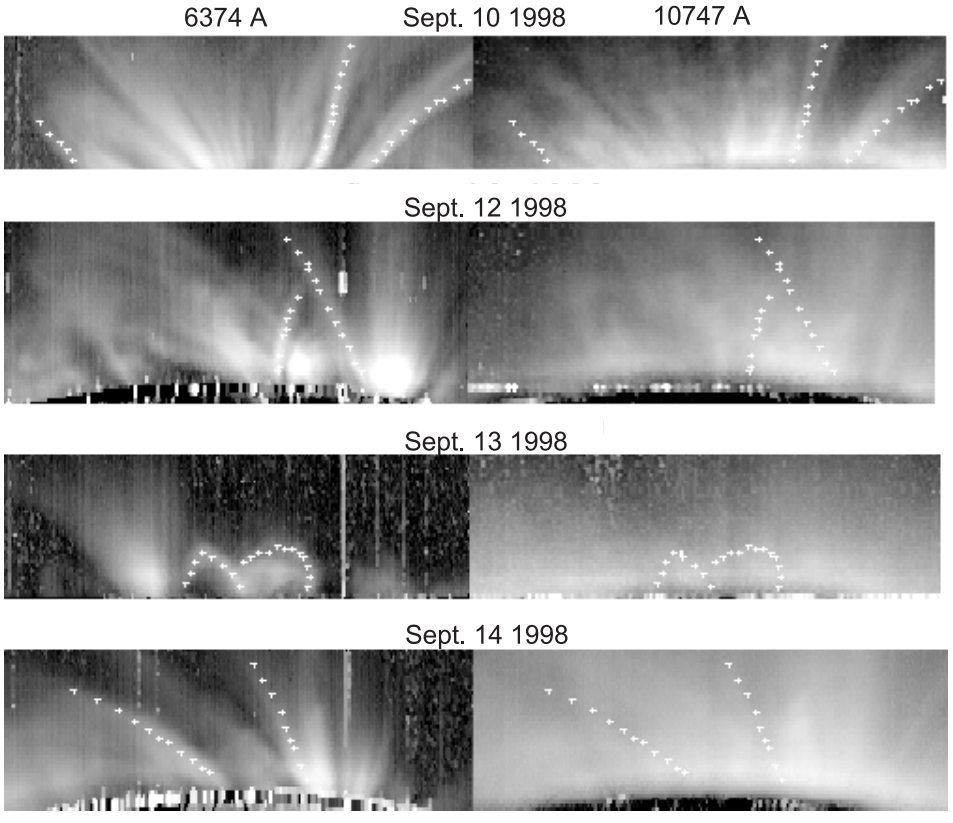

Figure 3. Same as for Fig. 1 but for 6374 Å and 10747 Å emission lines and variations in FWHM for the loops are shown in Fig. 7.

3. Results

Figure 4 shows that the line width of the [Fe XIV] 5303 Å emission line decreases with height above the limb in general and that of [Fe X] 6374 Å line increases with height above the limb. Line width of the [Fe XI] 7892 Å emission line also shows

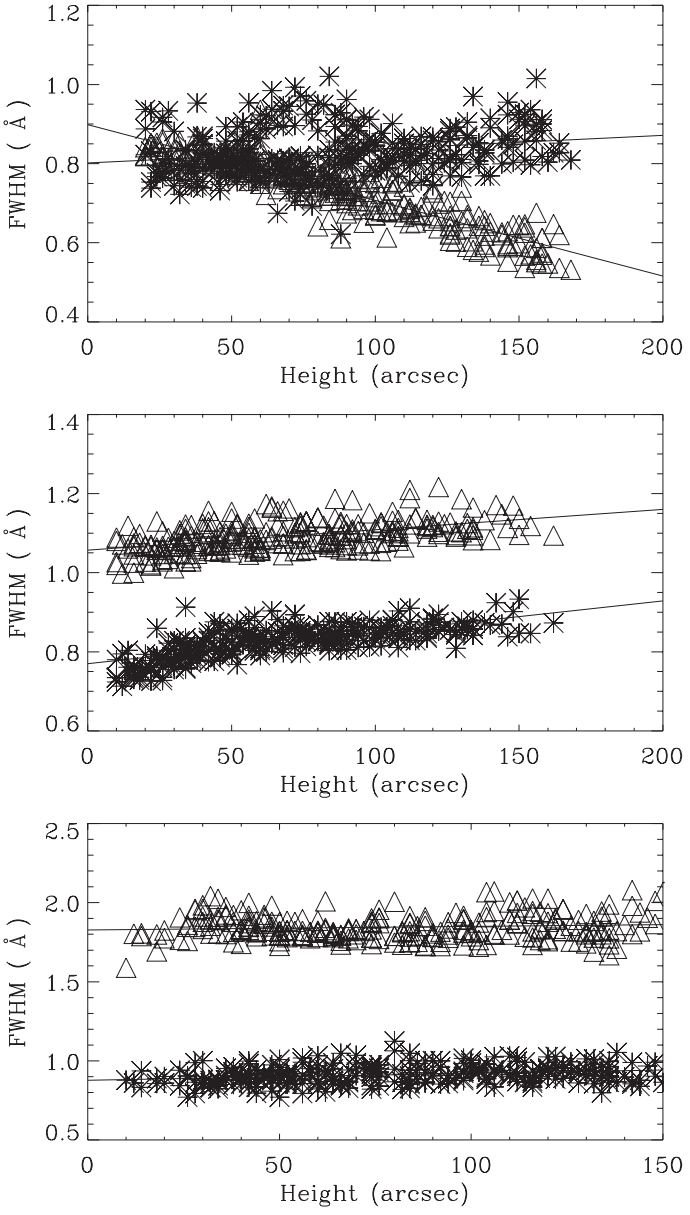

Figure 4. Top-most panel shows the variation of FWHM of the 6374 Å and 5303 Å emission lines with height above the limb when all the coronal loops in a coronal region are considered together. Middle panel shows the variations of 6374 Å and 7892 Å and bottom-most panel shows that of 6374 Å and 10747 Å emission lines.

increase with height but less steeply as compared to that for the 6374 Å line and the line width of [Fe XIII] 10747 Å shows marginal variations with height. We have analysed 1268 coronal loops observed in the 6374 Å line; 743 in the 5303 Å; 247 in the 7892 Å and 278 in the 10747 Å emission line. We found that 95% of the loops observed in 6374 Å line shows an increase in FWHM of the line with height above the limb; about 71% structures observed in 7892 Å line shows increase in FWHM with height; only 58% loops shows marginal increase in FWHM with height in 10747 Å line whereas 89% coronal loops shows decrease in FWHM with height above the limb in case of 5303 Å line. The increase in FWHM is maximum in case of 6374 Å emission line representing relatively low temperature plasma. Coronal loops of different sizes and shapes e.g., face-on and end-on; radial and non-radial; open and closed; were studied. Typical examples of the loops studied are shown by + marks in Figs. 1–3. Figure 5 shows the FWHM of the 6374 Å and 5303 Å emission lines

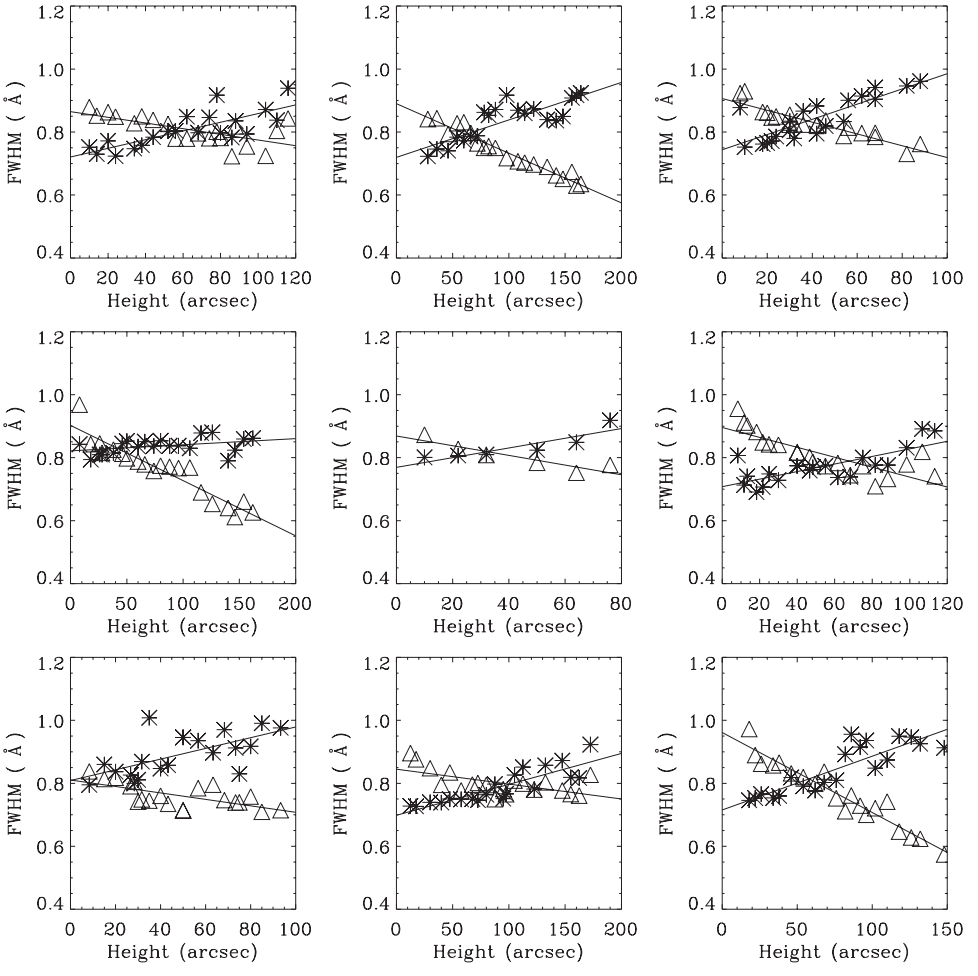

Figure 5. Nine panels show the variations of FWHM of 6374 Å and 5303 Å emission lines with height above the limb for various types of coronal loops shown in Fig. 1. The trend in variation of FWHM of 5303 Å line is the same in all the loops but the magnitude differs.

as a function of height in different types of loops. Figure 6 shows some other examples of the variation of FWHM in the 6374 Å and 7892 Å lines with height and Fig. 7 shows the same for 6374 Å and 10747 Å emission lines. The Figs. 5–7 indicate that the trend in the variations in FWHM with height for a chosen line is the same irrespective of the size, shape and orientation of the coronal loop. We also find that on an average, intensity ratio of 7892 Å to 6374 Å increases with height; that of 10747 Å to 6374 Å line remains almost unchanged with height and that of 5303 Å to 6374 Å decreases with height above the limb. Generally from the coronal loop models and abundances of ions as a function of temperature, one expects to observe a steeper increase in the intensity ratio of 5303 Å to 6374 Å as compared to that of 7892 Å to 6374 Å with height, opposite to the observed decrease in the intensity ratio with height.

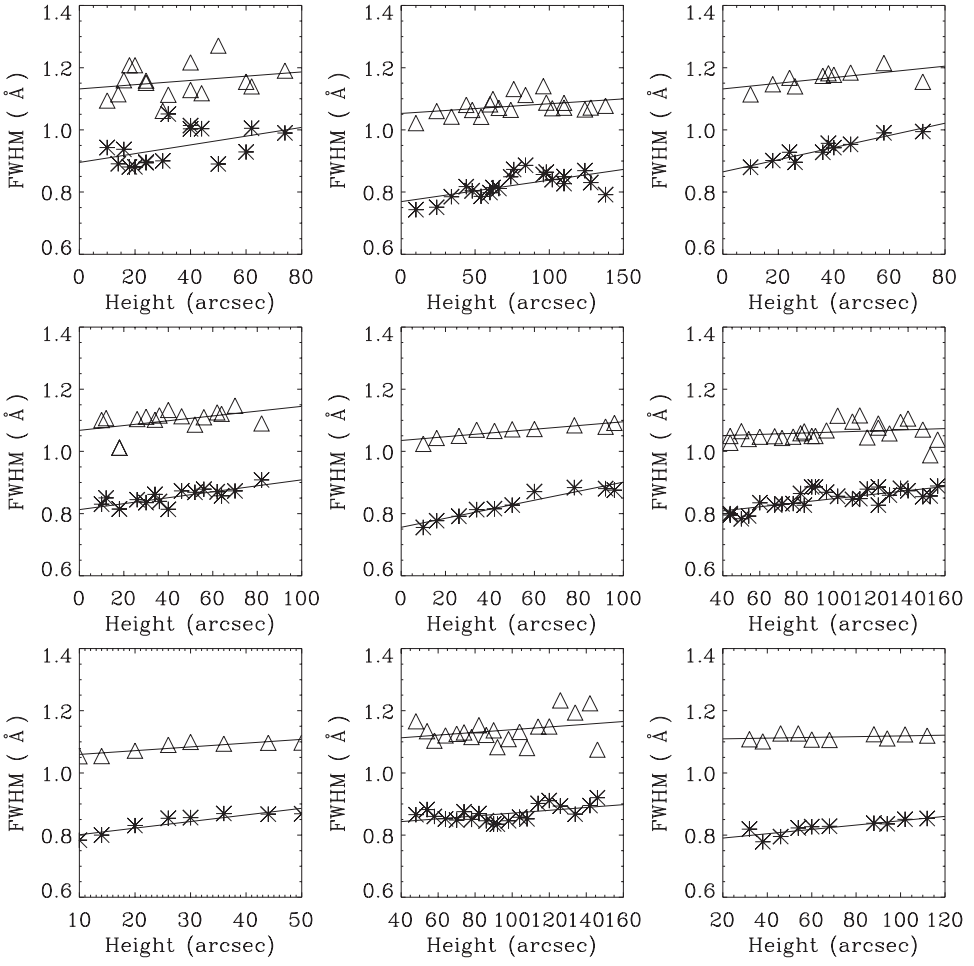

Figure 6. Same as that for Fig. 5 but for 6374 Å and 7892 Å emission lines and for coronal loops shown in Fig. 2.

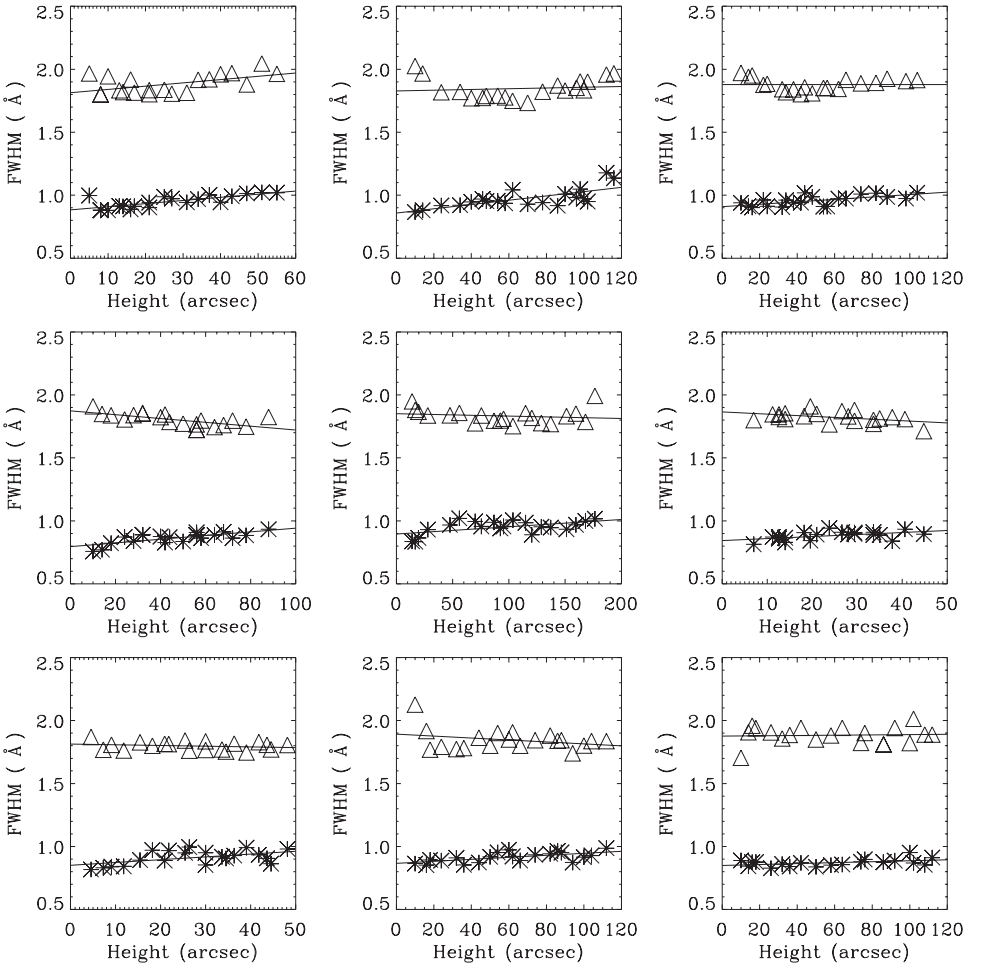

Figure 7. Same as that for Fig. 5 but for 6374 Å and 10747 Å emission lines and for coronal loops shown in Fig. 3.

4. Discussion and conclusion

These observations can be explained by assuming that the broad coronal loops connecting the magnetic field at the photospheric level and the fine structures in the corona are due to temperature and density variations in the broad loops and dynamic in nature. Probably plasma is fed in to these fine loops from the photosphere through chromosphere and the transition region and gets heated by small scale reconnections during its upward movement. The footpoints of the fine structures may be in different physical conditions leading to different temperature and density in the fine coronal loops. At larger heights the plasma in the fine structures interacts probably by collision and causes the relatively hotter plasma to share its energy with the relatively colder plasma. The effect of interaction of plasma goes on increasing with height above the limb. In the process, hotter plasma gets little cooler and cooler plasma gets little hotter and all the plasma in the coronal loop reaches a common average temperature around a

height of about 250 arcsec; the height depending on the activity and configuration of the coronal region and underlying magnetic fields. Under this assumption, we expect to observe an increase in the FWHM of the 6374 Å line and decrease in FWHM of 5303 Å line with height. We also expect to observe small variations in FWHM of 7892 Å and 10747 Å emission lines as these lines represent intermediate temperature plasma and thus will have smaller variations in temperature as compared to the variation of temperature in case of 6374 Å and 5303 Å line plasma. We also expect to observe an increase in the intensity ratio of 7892 Å to 6374 Å line as the temperature of plasma associated with both of these lines will increase in the loop with height and decrease in the intensity ratio of 5303 Å to 6374 Å line because temperature of the plasma representing 5303 Å line decreases with height. This scenario agrees with our findings. Therefore, the observed increase in FWHM with height above the limb of coronal emission lines associated with plasma at about 1 MK may not be due to increase in non-thermal motions caused by coronal waves but due to interaction with the relatively hotter plasma. These findings also do not support the existing coronal loop models, which predict an increase in temperature of the loop with height above the limb and put major restrictions on the loop models. New models need to be developed to explain the observations and those may include interaction of relatively hot and cold plasma.

References

Kano, R., Tsuneta, S. 1996, *Publ. Astron. Soc. Japan*, **48**, 535.
Porter, L. J., Klimchuk, J. A. 1995, *Astrophys. J.*, **454**, 499.
Rosner, R., Tucker, W. H., Vaiana, G. S. 1978, *Astrophys. J. Suppl.*, **220**, 643.
Serio, S., Peres, G., Vaiana, G. S., Golub, L., Rosner, R. 1981, *Astrophys. J.*, **243**, 288.
Singh, J., Ichimoto, K., Imai, H., Sakurai, T., Takeda, A. 1999, *Publ. Astron. Soc. Japan*, **51**, 269.
Singh, J., Ichimoto, K., Sakurai, T., Muneer, S. 2003a, *Astrophys. J.*, **585**, 516.
Singh, J., Sakurai, T., Ichimoto, K., Muneer, S. 2003b, *Solar Phys.*, **212**, 343.
Singh, J., Sakurai, T., Ichimoto, K., Watanabe, T. 2004, *Astrophys. J. Lett.*, **617**, L81.
Singh, J., Sakurai, T., Ichimoto, K., Suematsu, Y., Takeda, A. 2002, *Publ. Astron. Soc. Japan*, **54**, 793.
Tousey, R. *et al.* 1973, *Solar Phys.*, **33**, 265.
Tsubaki, T. 1975, *Solar Phys.*, **43**, 147.
Vaiana, G. S., Davis, J. M., Giacconi, R., Krieger, A. S., Silk, J. K., Timothy, A. F., Zombeck, M. 1973, *Astrophys. J.*, **185**, L47.
Winebarger, A. R., Warren, H. P., Mariska, J. T. 2003, *Astrophys. J.*, **587**, 439.